Colloid Polym Sci (2009) 287:933–942
DOI 10.1007/s00396-009-2049-5

ORIGINAL CONTRIBUTION

Drying dissipative structures of aqueous solution of poly(ethylene glycol) on a cover glass, a watch glass, and a glass dish

Tsuneo Okubo · Junichi Okamoto · Shinya Takahashi · Akira Tsuchida

Received: 16 March 2009 / Revised: 17 April 2009 / Accepted: 30 April 2009 / Published online: 26 May 2009

Abstract Drying dissipative structures of aqueous solution of poly(ethylene glycol) (PEG) of molecular weights ranging from 200 to 3,500,000 were studied on a cover glass, a watch glass, and a glass dish on macroscopic and microscopic scales. Any convectional and sedimentation patterns did not appear during the course of drying the PEG solutions. Several important findings on the drying patterns are reported. Firstly, the crystalline structures of the dried film changed from hedrites to spherulites as the molecular weight and/or concentration of PEG increased. Secondly, lamellae were formed along the ring patterns especially at high concentrations and high molecular weights. The coupled crystalline patterns of the spherulites and the lamellae were observed in a watch glass along the ring structures, supporting the important role of the convection by the gravity during the course of dryness. The coupled patterns were difficult to be formed on a cover glass and a glass dish, except at the outside edge of the dried film. Thirdly, the size of the broad ring at the outside edge of the dried film especially on a cover glass and a watch glass increased sharply as the molecular weight increased and also as the polymer concentration increased.

Keywords Poly(ethylene glycol) · Poly(ethylene oxide) · Dissipative structure · Drying pattern · Spherulite · Hedrite · Lamellae

Electronic supplementary material The online version of this article (doi:10.1007/s00396-009-2049-5) contains supplementary material, which is available to authorized users.

T. Okubo (✉)
Institute for Colloidal Organization,
Hatoyama 3-1-112, Uji,
Kyoto 611-0012, Japan
e-mail: okubotsu@ybb.ne.jp

J. Okamoto · S. Takahashi · A. Tsuchida
Department of Applied Chemistry, Gifu University,
Yanagido 1,
Gifu 501-1193, Japan

Introduction

In general, most structural patterns in nature form via self-organization accompanied with the *dissipation* of free energy and in the nonequilibrium state. In order to know the mechanisms of the dissipative self-organization of the simple model systems instead of the much complex nature itself, the authors have studied the *convectional*, *sedimentation*, and *drying* dissipative patterns during the course of drying colloidal suspensions and solutions as systematically as possible, though the three kinds of patterns are correlated strongly and overlapped each other [1, 2].

The most famous *convectional* pattern is the *hexagonal circulating* one, *Benard cell,* and has been observed when liquids contain plate-like colloidal particles as monitors and are heated homogeneously in a plain pan [3–5]. Another typical convectional pattern is the *Terada cell*, where the spoke-like lines prevail in the whole area at the liquid surface and are accompanied with the huge number of small *cell convections* in the normal direction of the spoke lines [6–9]. The Benard cells (but distorted greatly in many cases) and Terada cells were observed in the initial course of dryness of the Chinese black ink in a glass dish [10], the 100% ethanol suspensions of colloidal silica spheres [11], a cup of miso soup [12], coffee [13], black tea [14], and colloidal crystals of poly(methyl methacrylate) (PMMA) spheres on a cover glass and a watch glass [15, 16].

The whole growing processes of the convectional patterns are summarized as seven steps [10–16]. Firstly, at the initial stage of convection, appearance and disappearance of the

circulating lines (*irregular circulations*) take place at random in their direction accompanied with the *gravitational* upward transformation of heat. Secondly, global flow of the convection takes place at the surface layers from the center toward the outward edge of the liquid. Thirdly, the cooperated distorted Benard cells formed at the liquid surface. Fourthly, the reversed global flow of convection from the outside edge to the central area is observed at the liquid surface at the middle stage of convection. The reversal takes place mainly by the *Marangoni* convection. Fifthly, growing of the spoke lines from the outside edge to the central area takes place at the liquid surface layers. Sixthly, the clusters and further bundles of the spoke lines are formed at the final stage of convection. Growing of the broad ring-like sedimentation and drying patterns are formed in the middle and/or final stage of convections. The bundles at the final stage of convection are considered also to be the sedimentation ones and are further transformed to the drying patterns with fine structures. Seventhly, the convectional flow by the pinning effect proposed by Deegan et al. [17, 18] comes important at the final stage of convections.

Sedimentation dissipative patterns in a glass dish, a cover glass, a watch glass, and other substrates have been studied in detail in the course of drying suspensions of colloidal silica spheres (183 nm to 1.2 μm in diameter) [19–24], size-fractionated bentonite particles [25], green tea (Ocha) [26], and miso soup [12], for the first time, in our laboratory. The broad ring patterns were formed within 10 min in suspension state by the convectional flow of water and the colloidal particles. It was clarified that the sedimentary particles were suspended above the substrate by the electrical double layers and always moved by the balancing of the external force fields, including convectional flow and sedimentation. Furthermore, the sharpness of the broad rings was sensitive to the change in room temperature and/or humidity [21]. Quite recently, it was clarified that the dynamic bundle-like sedimentation patterns formed cooperatively from the spoke-line-like convectional structures of colloidal particles for coffee [13], black tea [14], and colloidal crystals of PMMA spheres [15, 16].

Drying dissipative patterns have been studied for suspensions and solutions of colloidal particles [1, 2, 10–13, 19–32], linear-type synthetic and bio-polyelectrolytes [33, 34], water-soluble neutral polymers [35, 36], ionic and nonionic detergents [37–39], gels [40], and dyes [41] mainly on a cover glass. The macroscopic broad ring patterns of the hill accumulated with the solutes in the outside edges formed on a cover glass, a watch glass, and a glass dish. The broad rings moved inward when solute concentration decreased and/or solute size increased. For the nonspherical particles, the round hill was formed in the center area in addition to the broad ring [25]. Macroscopic spoke-like cracks or fine hills, including flickering spoke-like ones, were also observed for many solutes. Furthermore, beautiful microscopic fractal patterns such as earthworm-like, branch-like, arc-like, block-like, star-like, cross-like, and string-like ones were observed. These microscopic drying patterns were often reflected from the *shape*, *size*, and/or *flexibility* of the solutes themselves. Microscopic patterns also formed by the translational Brownian diffusion of the solutes and the electrostatic and/or the hydrophobic interactions between solutes and/or between the solutes and the substrate in the course of solidification. One of the very important findings in our experiments is that the primitive vague sedimentation patterns were formed already in the liquid phase before dryness and they grew toward fine structures in the processes of solidification [25].

Deegan et al. [17, 18] have reported the traces of spoke-like patterns in the suspensions of polystyrene spheres (1 μm in diameter) under a microscope. They introduced the capillary flow theory accompanied with the *pinning* effect of the contact line of the drying drop. From our series of drying experiments for suspensions and solutions, however, the important role of the pinning effect was not always supported except in experiments at high particle concentrations and/or for small colloidal particles. In general, the broad ring-like drying patterns are always formed irrespective of the solutes and substrates used. However, they moved toward the central area and their size became small until the solute–solute *repulsive* or *attractive* interactions are strong enough to form the intersolute structures on substrates such as critical concentration of the structure formation of colloidal crystals [15, 16], biopolymer's helix and sheet structures [33], or detergent's micelles [37, 38]. Calchile et al. [42, 43] reported that the droplets of completely wetting liquids deposited on a thoroughly smooth and wetting surface for which no contact line anchoring occurs. The author believes that the convectional flow of solvent and solutes is essentially important throughout the convectional, sedimentation, and drying pattern formation. The pinning effect was not also supported in a glass dish, where drying frontier starts from the central area of a vessel substrate and developed toward outside. It should be mentioned that theoretical studies for the convectional patterns have been made intensively hitherto, but these are not always successful yet [17, 18, 44–51]. It should be further noted that information on the *size*, *shape*, *conformation*, and/or *flexibility* of particles and polymers, for example, is transformed cooperatively and further accompanied with the *amplification* and *selection* processes toward the succeeding sedimentation and drying patterns during the course of dryness of solutions and suspensions [34, 37–39].

In this work, drying dissipative patterns of poly(ethylene glycol) (PEG, which is also named as poly(ethylene oxide) or poly(oxyethylene)) having molecular weights from 200 to 3,500,000 have been studied on the macroscopic and microscopic scales. The authors reported the drying patterns of PEG on a cover glass previously [36]. One of the main purposes of this work is the clarification of the importance of the convectional flow on the *crystalline structural formation* in the drying patterns and the understanding of the mechanism of the broad rings at the outside edge of the dried film.

Experimental

Materials

Nine kinds of poly(ethylene glycol), PEG0.2K, PEG1K, PEG2K, PEG4K, PEG8K, PEG20K, PEG500K, PEG2000K, and PEG3500K having the average molecular weights of 180~220, 1,000, 2,000, 3,000, the exact value of molecular weight being not available, 20,000±5,000, 300,000~500,000, 1,500,000~2,000,000, and 3,000,000~3,500,000, as the manufacturers reported, respectively, were used without further purification. Eight samples except PEG8K were purchased from Wako Chemicals Co. (Tokyo). PEG8K was from MP Biomedicals, Inc. (Solon, OH, USA). The water used for the sample preparation was purified by a Milli-Q reagent-grade system (Milli-RO plus and Milli-Q plus, Millipore, Bedford, MA, USA).

Observation of the dissipative structures

The 0.1-ml aliquot of the aqueous solution of PEG sample was carefully and gently placed onto a micro cover glass (30×30 mm, no. 1, thickness 0.12 to 0.17 mm, Matsunami Glass, Kishiwada, Osaka, Japan) set in a plastic dish (type NH-52, 52 mm in diameter, 8 mm in depth, As One Co., Tokyo, Japan). The cover glass was used without further rinse. Four milliliters of the solution was set on a medium watch glass (70 mm, TOP Co. Tokyo, Japan). Five milliliters of the solution was put into a medium glass dish (42 mm in inner diameter and 15 mm in height, code 305-02, TOP Co.). The disposable serological pipettes (1 and 10 ml, Corning Lab. Sci., Co.) were used for putting the suspension in the substrates. The patterns during the course of dryness were observed for the solutions on a desk covered with a black plastic sheet. The room temperature was regulated at 24°C. The humidity of the room was not regulated and between 45% and 60%.

Macroscopic patterns were recorded on a Canon EOS 10 D digital camera with a macrolens (EF 50 mm, f=2.5) plus a life-size converter EF or a zoom lens (Canon, EF28-70 mm, 1:2.8) on a cover glass and a medium glass dish or a medium watch glass, respectively. Microscopic drying patterns were observed with a metallurgical microscope (PME-3, Olympus Co., Tokyo, Japan). Thickness profiles of the dried films were measured on a laser 3D profile microscope (type VK-8500, Keyence Co., Osaka, Japan). Polarizing microscopic pictures were taken on a Shimadzu polarizing microscope (Type Kalnew 53255, Shimadzu, Kyoto, Japan) with a charge-coupled device camera (Type TNC4604J, Kenis Ltd., Osaka, Japan).

Results and discussion

Macroscopic and microscopic drying patterns of PEG solutions on a cover glass

Figure 1 shows the typical macroscopic drying patterns of PEG solutions from PEG4K (line A) to PEG3500K (F) at concentrations from 0.003 monoM (line a) to 0.1 monoM (line d). The macroscopic patterns of PEG0.2K, PEG1K, and PEG2K were omitted in Fig. 1. For PEG0.2K, the final patterns were liquid-state broad rings at any concentrations. The sizes of the broad rings were very small and increased as polymer concentration increased. For PEG1K and 2K, the final patterns were *liquid* and *liquid* + *solid* coexistence at low and high polymer concentrations, respectively. The liquid-state areas coexisted with the solid pattern areas at 0.003 monoM even for PEG4K and PEG8K. The solid-state drying patterns were, however, observed at high concentrations. From PEG20K to PEG3500K, solid drying patterns were observed at any concentrations and areas as shown in Fig. 1. The broad ring patterns were always observed at the outside edge of the final patterns. Microscopic drying patterns such as spherulite and hedrite crystals were observed in the dried films, which will be described below in detail in the section of microscopic observation.

Figures 2 and 2a (in the "Electronic supplementary materials") shows the thickness profiles of the dried films as a function of the distance from the film center (r) at 0.03 monoM for PEG8K (a) to PEG3500K (e) and at 0.1 monoM for PEG20K (a) to PEG3500K (d), respectively. The profiles demonstrate the formation of the broad ring patterns clearly, and their size increased as the molecular weight of polymers increased. It should be noted that polymer accumulation takes place at the inner area of the broad ring for PEG of high molecular weight and concentration, though the thickness is much lower compared with the height of the broad ring (see panel d in Fig 2a (in the "Electronic supplementary materials"), for example). Recently, the whole processes of the convectional patterns

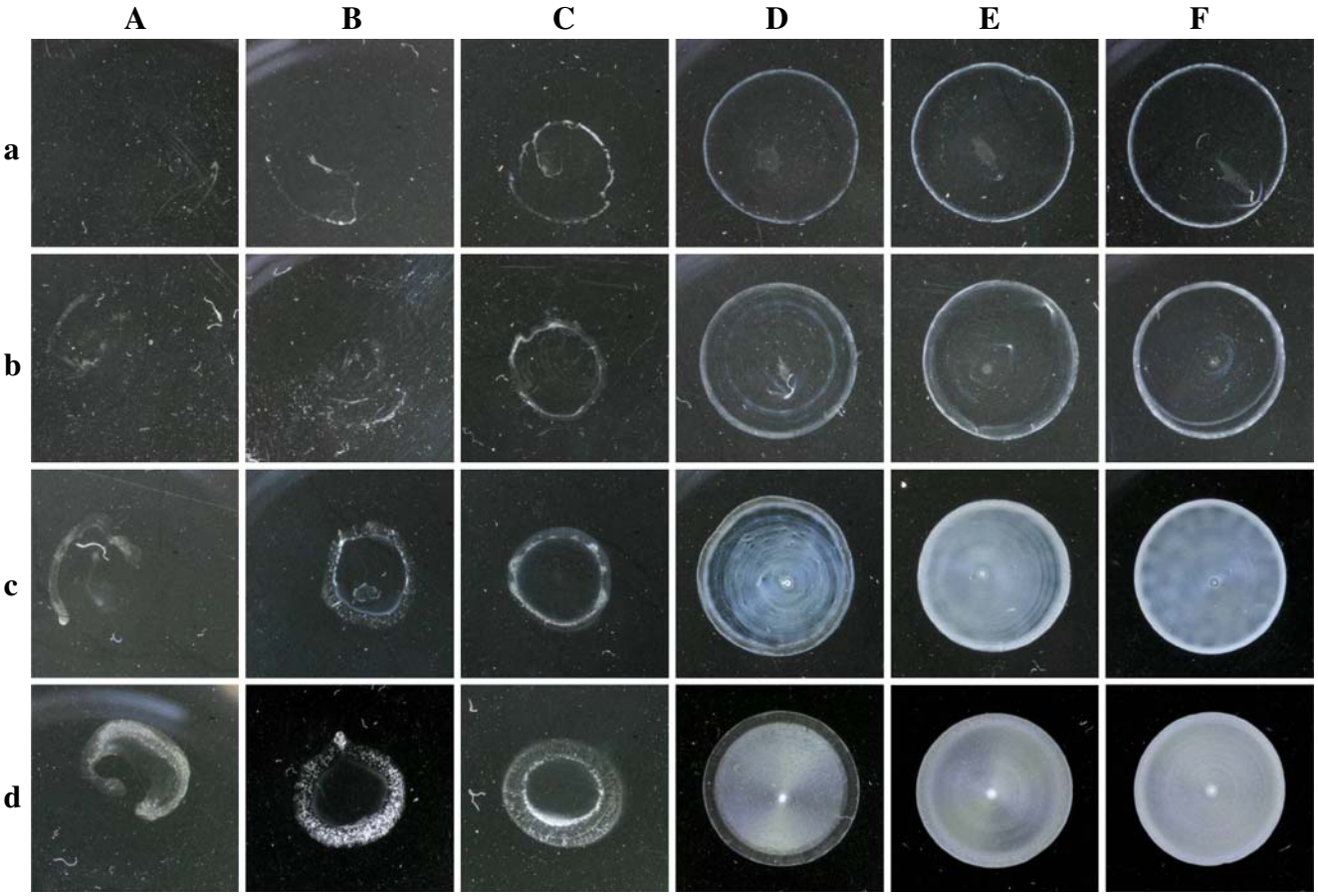

Fig. 1 Drying patterns of PEG solution on a cover glass at 24 °C. 0.1 ml, *A* PEG4K, *B* PEG8K, *C* PEG20K, *D* PEG500K, *E* PEG2000K, *F* PEG3500K, *a* 0.003 monoM, *b* 0.01 monoM, *c* 0.03 monoM, *d* 0.1 monoM

were summarized as seven steps as described in the "Introduction". The broad ring-like sedimentation patterns are formed in the convectional step four, where the reversal of the global flow takes place at the liquid surface. The ratios of the final size of the broad rings in diameter (d_f) against the initial size of the liquid in diameter (d_i) on a cover glass are shown in Fig. 3, where the d_f/d_i values in a watch glass were also displayed by solid circles. The size of the broad rings was measured as the distance between the outside positions, not the peak center positions of the broad rings. Clearly, the broad ring size increased sharply as the molecular weight of PEG increased. This is due to the fact that the interpolymer structure is formed at low polymer concentrations when the molecular weight of the polymer is high. As described already in the "Introduction", the broad ring size decreases until the solute–solute repulsions or attractions are strong enough to form the intersolute structures such as colloidal crystals [15, 16], helix or sheet structures [33], and detergent's micelles [37, 38]. It should be mentioned here that the change in the size of broad rings does not support the pinning effect of the contact line proposed by Deegan et al. [17, 18]. However, pinning effect plays an important role in the final stage of dryness. Quite recently, the authors observed that the small single crystal areas are formed by the pinning effect around the large crystals in aqueous solutions of sodium chloride (T. Okubo, publication in preparation).

Two typical microscopic pictures are displayed in Fig. 4a and 4b (in the "Electronic supplementary materials") for PEG0.2K (line A), PEG1K (B), PEG2K (C), PEG4K (D), PEG8K (E), PEG20K (F), PEG500K (G), PEG2000K (H), and PEG (I). Lines a, b, c, and d are the two typical pictures at the initial polymer concentrations of 0.003, 0.01, 0.03, and 0.1 monoM, respectively. For PEG0.2K, the liquid did not dry at room temperature to the solid state at any concentrations and areas. Furthermore, any fine microscopic structures were not observed in the liquid patterns. For PEG1K, the solid structures at 0.1 monoM look like *hedrites* as reported by Allen and Mandelkern [52], for example. Furthermore, the hedrites and/or intermediate crystalline structures between spherulites and hedrites were observed for PEG2K at 0.03 monoM, PEG4K at 0.01 to 0.1 monoM, and PEG8K and PEG20K at all the concentrations examined. On the other hand, the typical spherulite

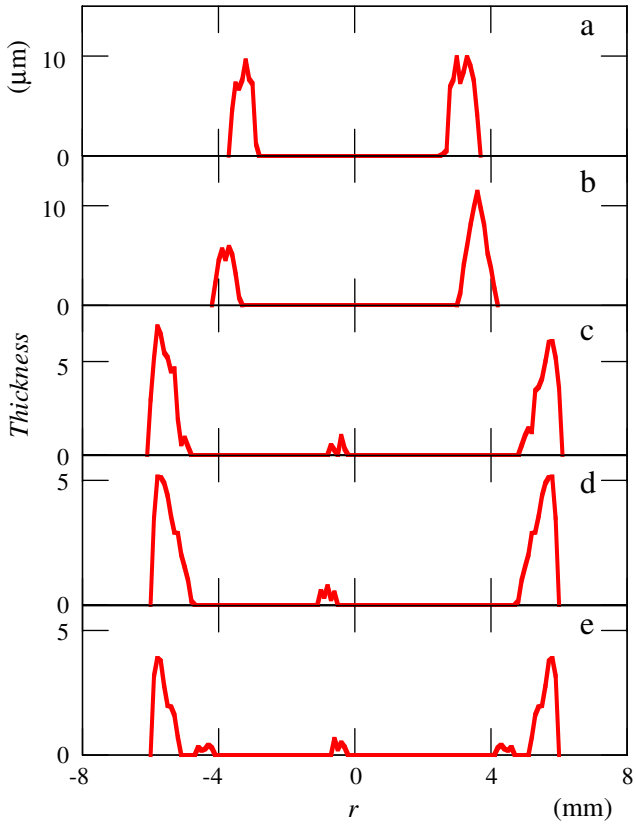

Fig. 2 Thickness profiles of the dried film of PEG solution on a cover glass as a function of the distance from the center at 24°C. 0.03 monoM, **a** PEG8K, **b** PEG20K, **c** PEG500K, **d** PEG2000K, **e** PEG3500K

crystalline structures were observed for PEG500K, PEG2000K, and PEG3500K on a cover glass. Much-extended microscopic pictures are shown in Fig. 4c for PEG500K to PEG3500K. The size of the spherulites was 50 to 200 μm. The spherulites were observed for PEG at

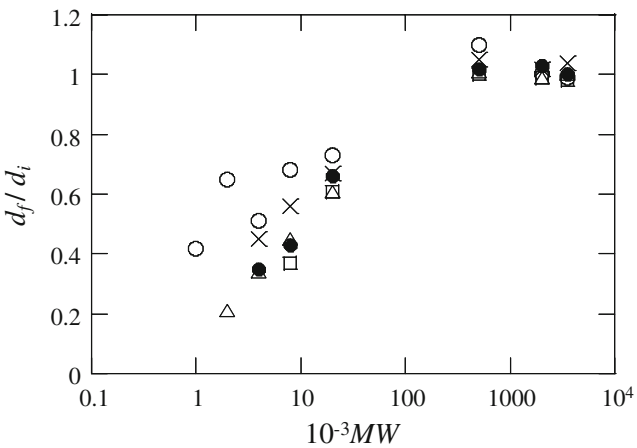

Fig. 3 Plots of d_f/d_i of PEG at 0.1 monoM (*open circles*), at 0.03 monoM (*crosses*), at 0.01 monoM (*open triangles*), and at 0.003 monoM (*open squares*) on a cover glass and at 0.01 monoM in a watch glass as a function of molecular weight

high molecular weights, 3.8×106 and greater [52]. The spherulite and hedrite structures of PEG have been studied in detail by other researchers [53–70] besides Allen and Mandelkern. It should be mentioned here that the typical spherulites were formed in the areas of the broad rings and also in central areas (see Fig. 4a, c, d, f, g, i). Furthermore, the lamella structures making the ring patterns macroscopically were formed in between the spherulites (see Fig. 4e, f, for example). Both the fine and broad ring structures were observed so often in the inner region of the broad ring at the outside edge of the dried film. It is highly plausible that the formation of the lamella structures is induced by the convectional flow in the course of dryness. It should be further mentioned that the spherulite patterns were not always perfect in their shape but cut by the outside broad ring lines (see Fig. 4f, i) and/or inner rings (see Fig. 4a, d, g). This supports that the crystallization on a cover glass is influenced significantly by the shearing forces induced by the convectional flow of the liquid in the course of dryness. Increase in the growing rates of the spherulites with shearing forces has been reported [67]. Further discussion of the shearing force effect is made in the section of dryness in a watch glass.

Figure 5a, b shows the typical pictures of the polarizing microscopy of PEG2000K at the central area of the drying film and at the outside edge, respectively. The Maltese cross patterns, especially at the central area, support the existence of the spherulite structure. However, the patterns are distorted to some extent, due to the collision and/or overlapping of the spherulites. The spherulite structures at the outside broad ring area are highly distorted by the substantial overlapping. It is highly plausible that the PEG polymers are undoubtedly accumulated densely.

Macroscopic and microscopic drying patterns of PEG solutions in a watch glass

Figure 6 shows the macroscopic patterns of PEG solutions from PEG0.2K to PEG3500K in a watch glass. For PEG0.2K, the whole patterns were liquid. Several findings are clear. Firstly, for PEG1K to PEG8K, the liquid areas coexisted with solid. For PEG20K to PEG3500K, the drying patterns were solid. These observations are similar to those on a cover glass. Secondly, the broad rings were observed for all the samples, and their sizes increased as the molecular weights increased, i. e., the diameters were 25, 25, 28, 24, 23, 36, 49, 50, and 52 mm from PEG0.2K to 3500K. Thirdly, the macroscopic spoke lines and ring patterns were observed as the molecular weights increased. Fourthly, the iridescent metallic colors appeared in the solid drying patterns. Fifthly, the polymers were vacant in the center area of the watch glass. Furthermore, the drying time (time required for the dryness) increased as the molecular

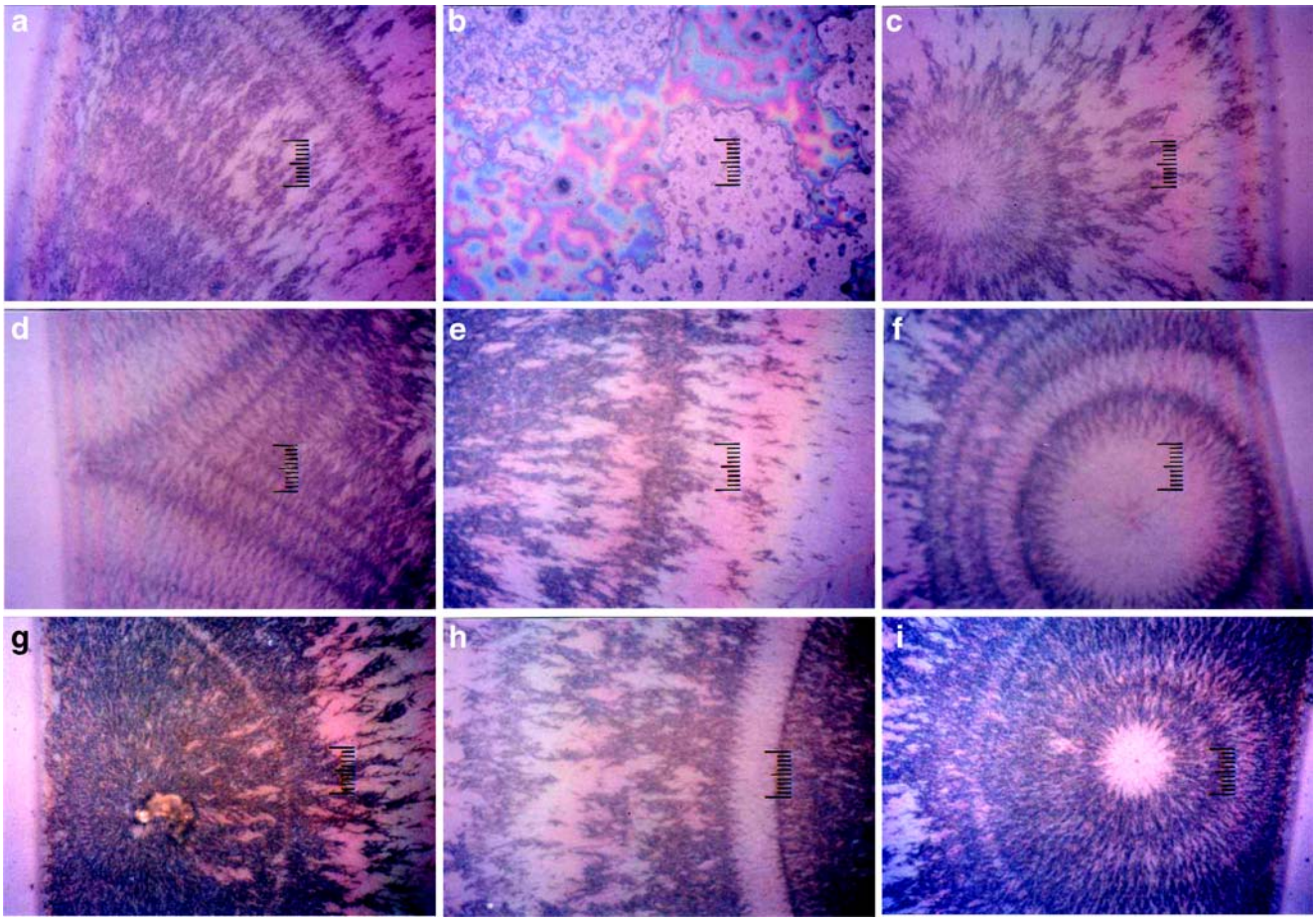

Fig. 4 Typical microscopic drying patterns of PEG solution on a cover glass at 24°C. **a**–**c** PEG500K, from center to right edge, **d**–**f** PEG2000K, **g**–**i** PEG3500K, 5 h 25 m after setting, 0.003 monoM, 0.1 ml; full scale is 25 μm

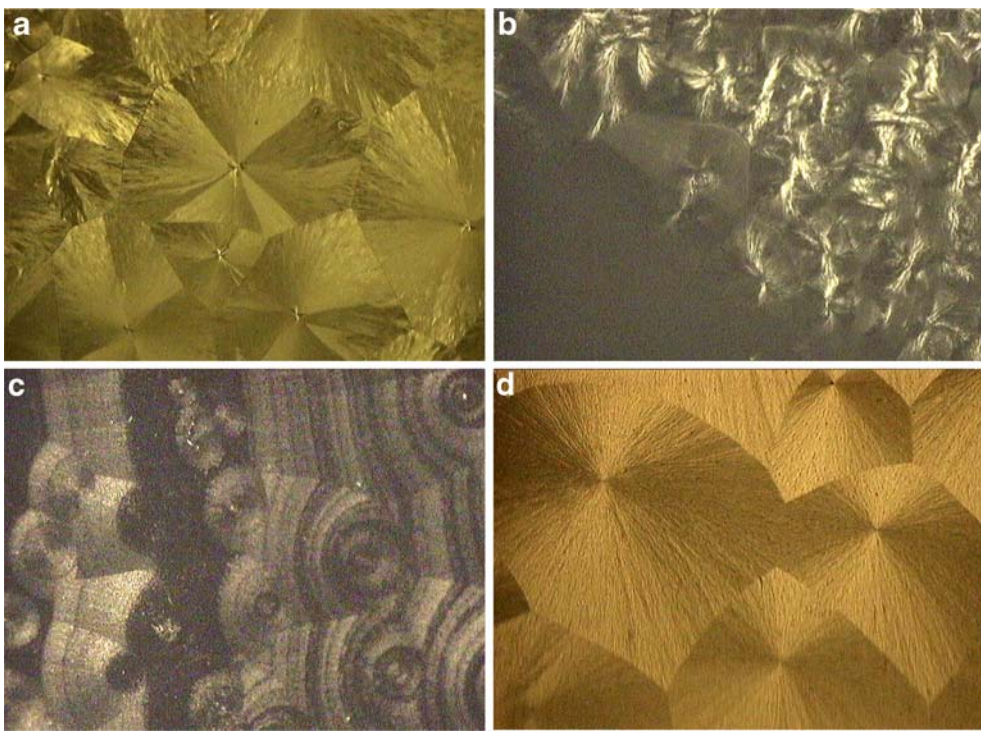

Fig. 5 Polarizing microscopic drying patterns of PEG solution on a cover glass (**a**, **b**), a watch glass (**c**), and a glass dish (**d**) at 24°C. **a** PEG200K, 0.1 monoM, central area, frame length 1.0×1.4 mm, **b** PEG2000K, 0.1 monoM, outside edge area, 0.26 ×0.34 mm, **c** PEG2000K, 0.1 monoM, 2.6×3.4 mm, **d** PEG3500K, 0.01 monoM, 1.0×1.4 mm

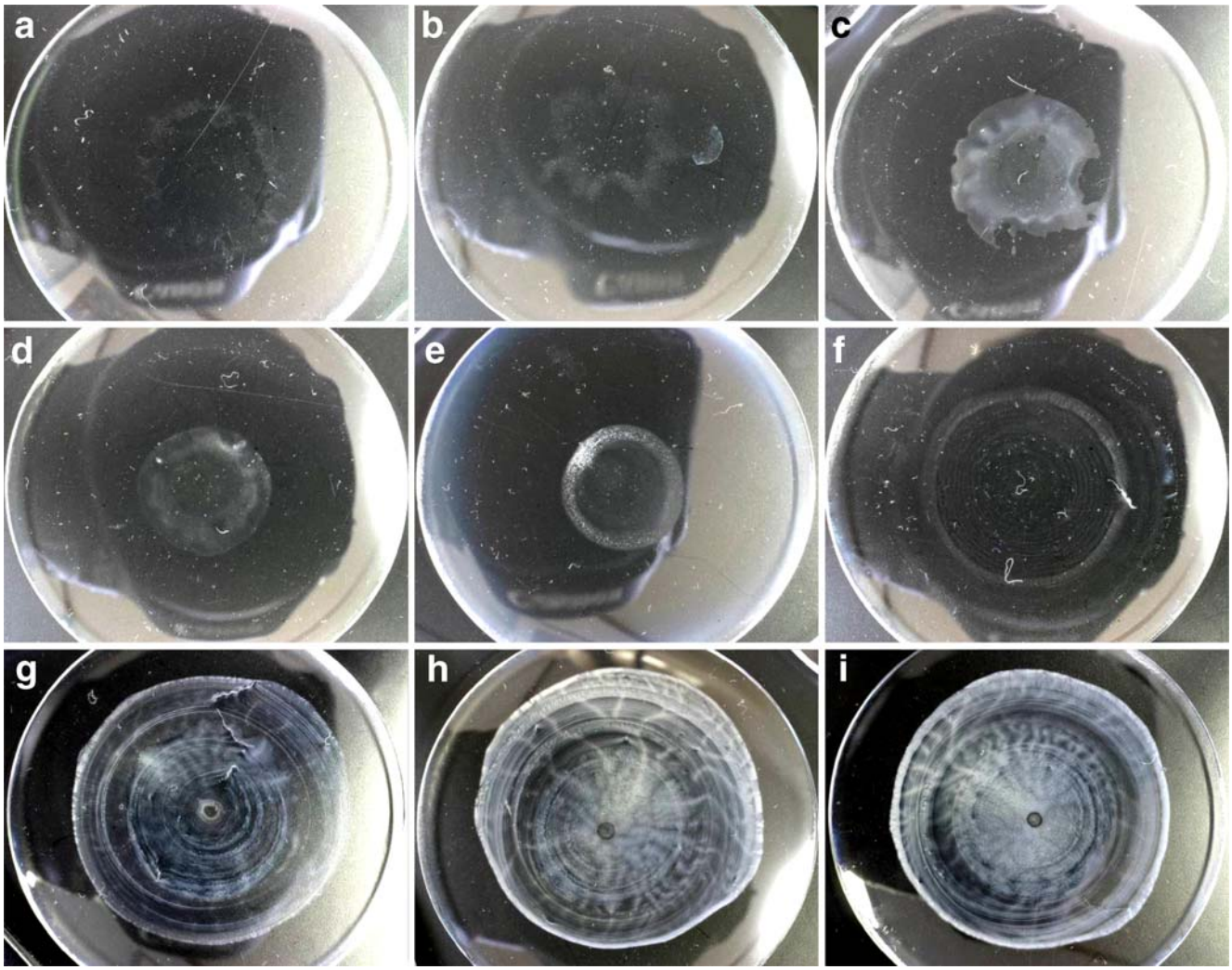

Fig. 6 Drying patterns of PEG solution on a watch glass at 24 °C. 0.01 monoM, 4 ml, **a** PEG0.2K, **b** PEG1K, **c** PEG2K, **d** PEG4K, **e** PEG8K, **f** PEG20K, **g** PEG500K, **h** PEG2000K, **i** PEG3500K

weight increased, though the graphs showing this were omitted in this report.

The microscopic pictures were compiled in Fig. 7a and 7b (in the "Electronic supplementary materials") and Fig. 7 for PEG0.2K to PEG2K, PEG4K to PEG20K, and PEG500K to PEG3500K, respectively, at 0.01 monoM of polymer concentration. For PEG0.2K, the final patterns remained in liquid state and did not dry up at any areas of the watch glass. Any fine patterns are, therefore, not observed. For PEG1K, hedrite patterns were observed in the pictures e and f of Fig. 7a (in the "Electronic supplementary materials"). The microscopic fine patterns i to k of PEG2K were also hedrite. The rather clear hedrite drying patterns were observed for PEG4K to PEG20K, though the liquid-state areas still remained in part (see picture l of Fig. 7b). It should be further noted in Fig. 7b that the fine microscopic ring patterns also coexisted with the hedrites as displayed in picture k of Fig. 7b (in the "Electronic supplementary materials").

For PEG500K to PEG3500K, clear-cut spherulite patterns, which coexisted with the lamellae lines, were observed (see Fig. 7). These lamellae lines originated from the ring structures, which have been observed so often in a watch glass hitherto [2, 11–13, 16, 19, 21, 23, 24, 26, 71]. Interestingly, the spherulite and the lamellae line structures were coupled to each other at the inner and outer areas of the watch glass as clearly shown in the pictures c and h to k of Fig. 7. The polarizing picture of Fig. 5c also supports the coupling of the two structures. It should be noted that these coupling patterns were seldom observed in a cover glass and a glass dish besides the outside edge of the dried films. These coupling phenomena further support the fact that the shearing forces induced during the dryness of the solutions play an important role in the pattern formation. The sloped

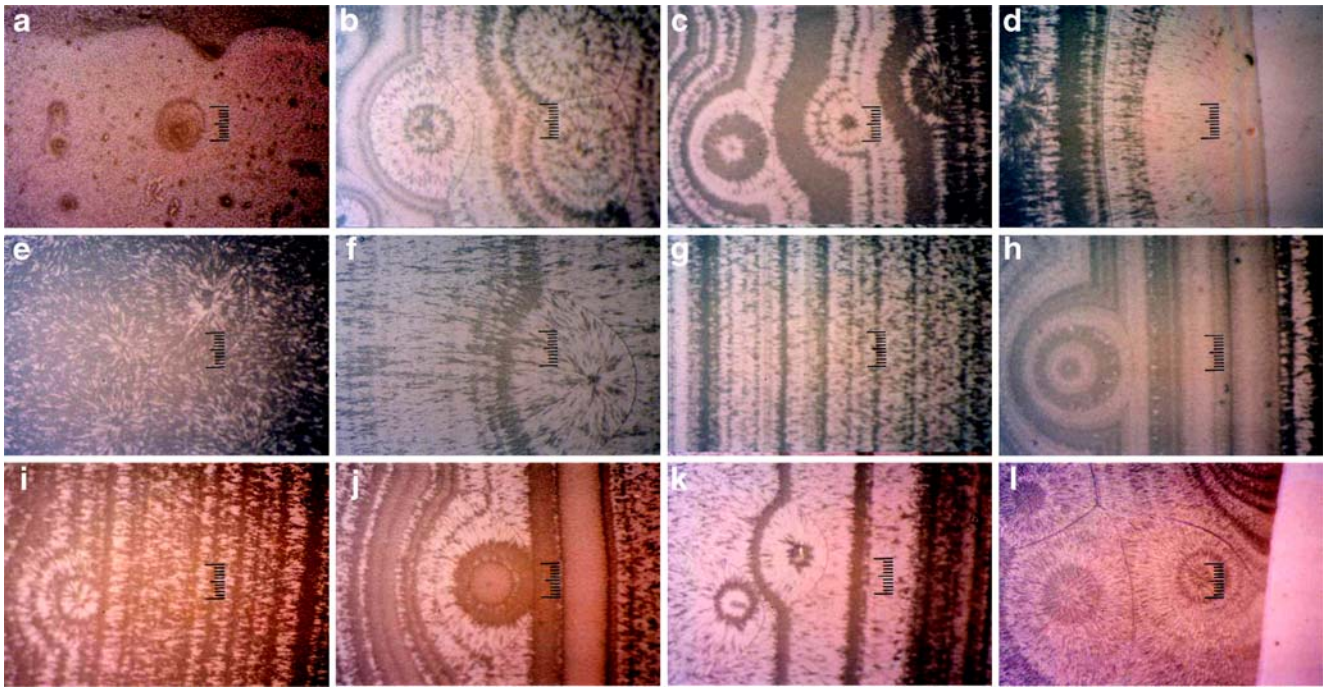

Fig. 7 Microscopic drying patterns of PEG solution in a watch glass at 24°C. **a**–**d** PEG500K, from center to right edge, **e**–**h** PEG2000K, **i**–**l** PEG3500K, 45 h25 m after setting, 0.01 monoM, 4 ml; full scale is 100 μm

glass wall of the watch glass must be effective to form the fine ring formation and the coupled structures.

Macroscopic and microscopic drying patterns of PEG solutions in a glass dish

The macroscopic drying patterns of aqueous solutions from PEG4K to PEWG3500K are shown in Fig. 8. Broad ring was observed for PEG polymers of molecular weights higher than 500 K. For the low molecular weight polymers, the final films were transparent and hard to recognize clearly in the pictures. It should be noted here that the broad rings in a glass dish were very broad compared with those on a cover glass and/or a watch glass. These observations support that the global convectional flow of the solvent water and the polymer solutes in a glass dish are not so regular and strong compared with those on a cover glass and/or a watch glass. Furthermore, the difference in the directions of the drying frontiers between outward in a glass dish and inward on a cover glass will be one of the important factors for the broadness.

Figure 9a (in the "Electronic supplementary materials") and Fig. 9 show the typical microscopic patterns of PEG4K to PEG20K and from PEG500K to PEG3500K in a glass dish, respectively. Surprisingly, any crystalline microscopic patterns were not observed for PEG4K to PEG20K. As described in the previous sections, these polymers showed hedrite crystalline structures on a cover glass and a watch glass. For PEG500K, the hedrite crystalline structures appeared around the central area (see Fig. 9a). The spherulite crystalline structures, on the other hand, formed easily at the outside area. For PEG2000K to PEG3500K, crystallization was difficult in the central area and the spherulites were formed also at the outside area. These observations are also related to the regularity of the global flow.

Concluding remarks

In this work, drying dissipative patterns of aqueous solutions of poly(ethylene glycol) having molecular weights from 200 to 3,500,000 were studied on a cover glass, a watch glass, and a glass dish on macroscopic and microscopic scales. Several important results were obtained. Firstly, the crystalline structures of the dried film changed from hedrites to spherulites as molecular weight and/or PEG concentration increased. Secondly, lamellae were formed along the ring patterns especially at high concentrations and molecular weights. The coupled patterns of the spherulites and the lamellae were formed especially in a watch glass, whereas the coupled patterns were difficult to observe on a cover glass and a glass dish except at the outside edge of the dried film. The formation of the coupled patterns supports the important role of the gravitational and Marangoni convections during the course of dryness. Thirdly, the broad ring size especially in a watch glass increased

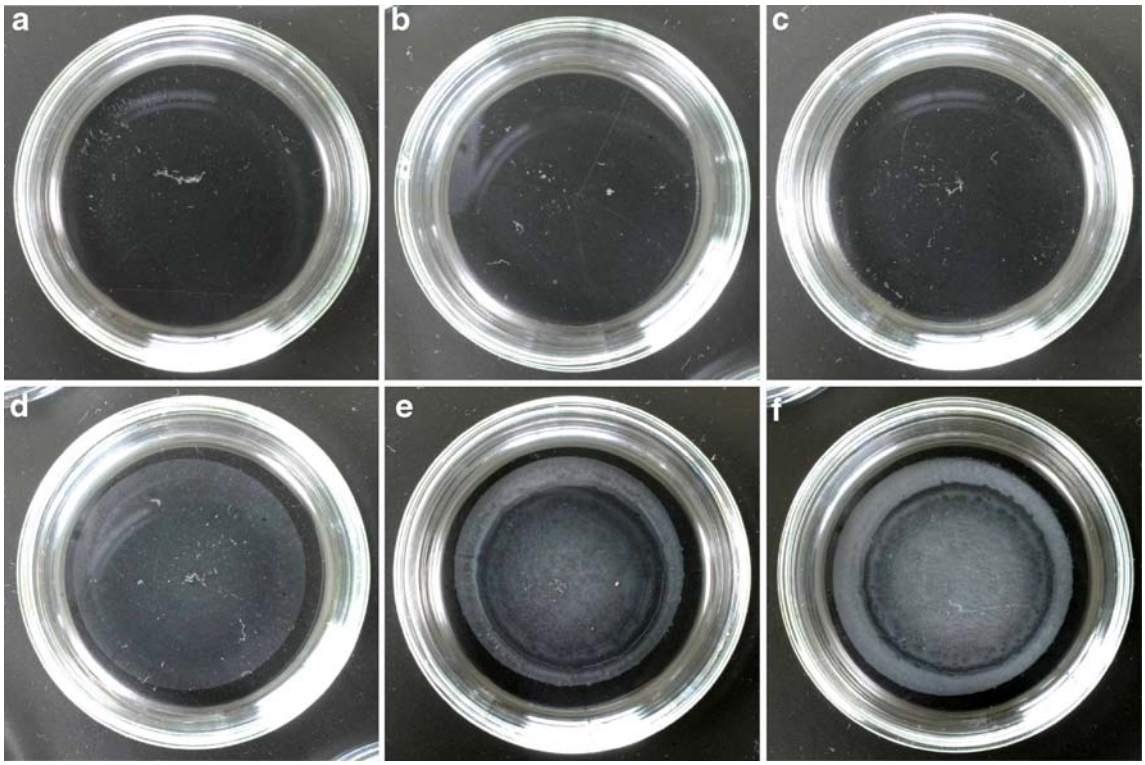

Fig. 8 Drying patterns of PEG solution in a glass dish at 24°C. 0.01 monoM, 5 ml, **a** PEG4K, **b** PEG8K, **c** PEG20K, **d** PEG500K, **e** PEG2000K, **f** PEG3500K

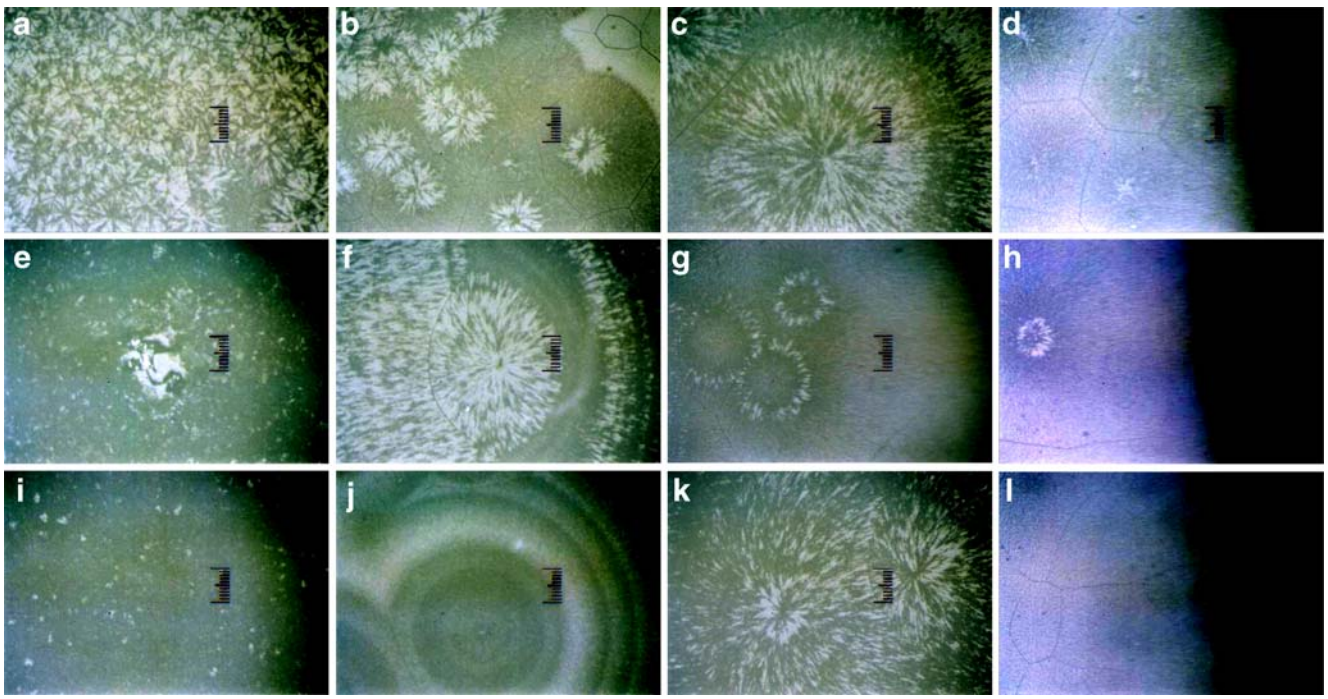

Fig. 9 Microscopic drying patterns of PEG solution in a glass dish at 24°C. **a**–**d** PEG500K, from center to right edge, **e**–**h** PEG2000K, **i**–**l** PEG3500K, 45 h25 m after setting, 0.01 monoM, 5 ml; full scale is 100 μm

sharply as the molecular weight increased and also as the polymer concentration increased.

Acknowledgments Professor Emeritus Keisuke Kaji of Kyoto University is highly acknowledged for his valuable comments on this work. Financial supports from the Ministry of Education, Culture, Sports, Science, and Technology, Japan and Japan Society for the Promotion of Science are greatly acknowledged for Grants-in-Aid for Exploratory Research (17655046 to T.O.) and Scientific Research (B; 18350057 to T.O. and 19350110 to A.T.).

References

1. Okubo T (2006) In: Stoylov SP, Stoimenova MV (eds) Molecular and colloidal electro-optics. Taylor & Francis, New York, p 573
2. Okubo T (2008) In: Nagarajan R, Hatton TA (eds) Nanoparticles: syntheses, stabilization, passivation and functionalization. ACS Book, Washington, DC, p 256
3. Gribbin G (1999) Almost everyone's guide to science. The universe, life and everything. Yale University Press, New Haven
4. Ball P (1999) The self-made tapestry. Pattern formation in nature. Oxford University Press, Oxford
5. Okubo T (2001) Beautiful world of colloids and interfaces (Japanese). Matsuo, Gifu
6. Terada T, Yamamoto R, Watanabe T (1934) Sci Paper Inst Phys Chem Res Jpn 27:173 Proc Imper Acad Tokyo 10:10
7. Terada T, Yamamoto R, Watanabe T (1934) Sci Paper Inst Phys Chem Res Jpn 27:75
8. Terada T, Yamamoto R (1935) Proc Imper Acad Tokyo 11:214
9. Nakaya U (1947) Memoirs of Torahiko Terada (Japanese). Kobunsya, Tokyo
10. Okubo T, Kimura H, Kimura T, Hayakawa F, Shibata T, Kimura K (2005) Colloid Polym Sci 283:1
11. Okubo T (2006) Colloid Polym Sci 285:225
12. Okubo T (2009) Colloid Polym Sci 287:167
13. Okubo T, Okamoto J, Tsuchida A (2009) Colloid Polym Sci 287:351
14. Okubo T, Okamoto J, Tsuchida A (2009) Colloid Polym Sci. doi:10.1007/s00396-009-2021-4
15. Okubo T, Okamoto J, Tsuchida A (2008) Colloid Polym Sci 286:1123
16. Okubo T (2008) Colloid Polym Sci 286:1307
17. Deegan RD, Bakajin O, Dupont TF, Huber G, Nagel SR, Witten TA (1997) Nature 389:827
18. Deegan RD, Bakajin O, Dupont TF, Huber G, Nagel SR, Witten TA (2000) Phys Rev E 62:756
19. Okubo T (2006) Colloid Polym Sci 284:1191
20. Okubo T (2006) Colloid Polym Sci 284:1395
21. Okubo T, Okamoto J, Tsuchida A (2007) Colloid Polym Sci 285:967
22. Okubo T (2007) Colloid Polym Sci 285:1495
23. Okubo T, Okamoto J, Tsuchida A (2008) Colloid Polym Sci 286:385
24. Okubo T, Okamoto J, Tsuchida A (2008) Colloid Polym Sci 286:941
25. Yamaguchi T, Kimura K, Tsuchida A, Okubo T, Matsumoto M (2005) Colloid Polym Sci 283:1123
26. Okubo T (2006) Colloid Polym Sci 285:331
27. Vanderhoff JW (1973) J Polym Sci Symp 41:155
28. Nicolis G, Prigogine I (1977) Self-organization in non-equilibrium systems. Wiley, New York
29. Ohara PC, Heath JR, Gelbart WM (1997) Angew Chem 109:1120
30. Maenosono S, Dushkin CD, Saita S, Yamaguchi Y (1999) Langmuir 15:957
31. Nikoobakht B, Wang ZL, El-Sayed MA (2000) J Phys Chem 104:8635
32. Ung T, Litz-Marzan LM, Mulvaney P (2001) J Phys Chem B 105:3441
33. Okubo T, Onoshima D, Tsuchida A (2007) Colloid Polym Sci 285:999
34. Okubo T, Kanayama S, Ogawa H, Hibino M, Kimura K (2004) Colloid Polym Sci 282:230
35. Shimomura M, Sawadaishi T (2001) Curr Opin Coll Interf Sci 6:11
36. Okubo T, Yamada T, Kimura K, Tsuchida A (2006) Colloid Polym Sci 284:396
37. Kimura K, Kanayama S, Tsuchida A, Okubo T (2005) Colloid Polym Sci 283:898
38. Okubo T, Shinoda C, Kimura K, Tsuchida A (2005) Langmuir 21:9889
39. Okubo T, Kanayama S, Kimura K (2004) Colloid Polym Sci 282:486
40. Okubo T, Emi I, Tsuchida A, Kokufuta E (2006) Colloid Polym Sci 285:339
41. Okubo T, Yokota N, Tsuchida A (2007) Colloid Polym Sci 285:1257
42. Cachile M, Benichou O, Cazabat AM (2002) Langmuir 18:7985
43. Cachile M, Benichou O, Poulard C, Cazabat AM (2002) Langmuir 18:8070
44. Palmer HJ (1976) J Fluid Mech 75:487
45. Anderson DM, Davis SH (1995) Phys Fluids 7:248
46. Pouth AF, Russel WB (1998) AIChEJ 44:2088
47. Burelbach JP, Bankoff SG (1998) J Fluid Mech 195:463
48. Matar OK, Craster RV (2001) Phys Fluids 13:1869
49. Hu H, Larson RG (2002) J Phys Chem B 106:1334
50. Rabani E, Reichman DR, Geissler PL, Brus LE (2003) Nature 426:271
51. Fischer BJ (2002) Langmuir 18:60
52. Allen RC, Manderkern L (1982) J Polym Sci Polym Phys Ed 20:1465
53. Hay JN, Sabir M, Steven RLT (1969) Polymer 10:187
54. Godovsky YK, Slonimsky GL, Garbar NM (1972) J Polym Sci 38:1
55. Maclaine JQG, Booth C (1975) Polymer 16:191
56. Jadrague D, Fatou JG (1977) Anal Quimica 73:639
57. Mihailov M, Nedkov E, Goshev I (1978) J Macromol Sci Phys B 15:313
58. Yang M, Salovey R, Allen SD (1990) J Polym Sci B Polym Phys 28:245
59. Mandelkern L (2004) Crystallization of Polymers, 2nd ed., Vol. 2. Cambridge
60. Da Costa VM, Fiske TG, Coleman LB (1994) J Chem Phys 101:2746
61. Huang T, Rey AD, Kamal MR (1994) Polymer 35:5434
62. Schultz JM, Miles MJ (1998) J Polym Sci B Polym Phys 36:2311
63. Gu F, Bu H, Zhang Z (2000) Polymer 41:7605
64. Park C, Robertson RE (2001) Polymer 42:2597
65. Sasaki T, Miyazaki A, Sugiura S, Okada K (2002) Polym J 34:794
66. Kawashima K, Kawano R, Miyagi T, Umemoto S, Okui N (2003) J Macromol Sci B Phys 42:889
67. Jiang SAL, Jiang B (2004) J Polym Sci B Polym Phys 42:656
68. Hobbs JK, Vasilev C, Humphris ADL (2005) Polymer 46:10226
69. Yang H, Yin W, Zhang X, Cai Z, Wang Z, Cheng R (2005) J Appl Polym Sci 96:2454
70. Machado JC, Silva GG, De Oliveira FC, Lavall RL, Rieumont J, Licinio P, Windmoller D (2007) J Polym Sci B Polym Phys 45:2400
71. Okubo T (2008) Colloid Polym Sci 286:1411